Geosci. Model Dev. Discuss., https://doi.org/10.5194/gmd-2018-58
Manuscript under review for journal Geosci. Model Dev.
Discussion started: 27 March 2018

Geoscientific Model Development Discussions

SHaKTI: Subglacial Hydrology and Kinetic Transient Interactions v1.0

Aleah Sommers[1], Harihar Rajaram[1], and Mathieu Morlighem[2]

[1]Department of Civil, Environmental, and Architectural Engineering, University of Colorado, Boulder, Colorado, USA
[2]Department of Earth System Science, University of California, Irvine, California, USA

Correspondence to: Aleah Sommers (aleah.sommers@colorado.edu)

Abstract. Subglacial hydrology has a significant influence on ice sheet dynamics, yet remains poorly understood. Complex feedbacks play out between the liquid water and the ice, with constantly changing drainage geometry and flow mechanics. A clear tradition has been established in the subglacial hydrology modeling literature of distinguishing between channelized (efficient) and distributed (inefficient) drainage systems or components. Imposing a distinction that changes the governing physics under different flow regimes, however, may not allow for the full array of drainage characteristics to arise. Here, we present a new subglacial hydrology model: SHaKTI (Subglacial Hydrology and Kinetic Transient Interactions). In this model formulation, a single set of governing equations is applied over the entire domain, with a spatially and temporally varying transmissivity that allows for representation of the wide transition between turbulent and laminar flow, and the geometry of each element is allowed to evolve accordingly to form sheet and "channel" configurations. The model is implemented as a solution in the Ice Sheet System Model (ISSM). We include steady and transient examples to demonstrate features and capabilities of the model, and we are able to reproduce seasonal behavior of the subglacial water pressure that is consistent with observed seasonal velocity behavior in many Greenland outlet glaciers, supporting the notion that subglacial hydrology may be a key influencer in shaping these patterns.

1 Introduction

One of the significant consequences of contemporary climate change is rising sea level. A large component of sea level rise is due to the transfer of ice from glaciers and ice sheets into the ocean via melt, runoff, and iceberg calving (IPCC, 2013). Although massive outlet glaciers of West Antarctica may be on the verge of irreversible collapse in the next 200 to 1,000 years (Joughin et al., 2014; DeConto and Pollard, 2016), the Greenland ice sheet is currently the single largest contributor to sea level rise (Shepherd et al., 2012). Considering the substantial amount of water held in this frozen reservoir (equivalent to approximately 7 m of sea level rise), it is important to improve understanding of its behavior, including the subtleties of its drainage, which affects ice velocity. Future ice dynamics remains a major uncertainty in sea level rise predictions (IPCC, 2013).

Since 1990, many Greenland outlet glaciers have displayed dramatic accelerations and frontal retreats, yielding substantial changes on the rapid timescale of decades or years, rather than centuries or millennia (Joughin et al. 2010). Other glaciers,

Geosci. Model Dev. Discuss., https://doi.org/10.5194/gmd-2018-58
Manuscript under review for journal Geosci. Model Dev.
Discussion started: 27 March 2018

Geoscientific Model Development Discussions
Open Access
EGU

however, have accelerated less rapidly or even decelerated over the same period (McFadden et al. 2011), and the mechanisms driving these contrasting responses are still not entirely understood. The recent accelerations observed in marine terminating outlet glaciers, which exhibit some of the greatest accelerations and are highly sensitive to changes in terminus conditions, may be in response to changing ocean temperatures (Nick et al. 2009, Rignot et al. 2010, Andresen et al. 2011). In land terminating glaciers, however, the observed accelerations are likely driven largely by liquid water inputs to the ice sheet from the surface via crevasses and moulins. Meltwater inputs have been shown to drive variation in ice velocities (e.g., Zwally et al., 2002; Bartholomew et al. 2012), as well as seasonal changes in the efficiency of the subglacial drainage system (Cowton et al. 2013).

In a recent update on the status of Greenland hydrology, Nienow et al. (2017) commented on our limited understanding of certain aspects of the Greenland hydrological system. The hydrology of meltwater on the surface, within, and beneath the Greenland ice sheet should ideally be viewed and modeled as a complex system of processes, considering the interconnectedness of surface mass balance, meltwater retention, discharge at the ice margin, and feedbacks between hydrology and ice dynamics (Rennermalm et al., 2013). These pieces are inextricably connected, but there also remain significant gaps in our understanding of the individual components. Water delivered to the bed through englacial conduits drives basal sliding, which has important effects on flow in some regions (Vaughan et al., 2013), and year-round sliding can occur with temperate bed conditions (Colgan et al., 2011). Increased meltwater input to the bed, however, does not necessarily imply increased basal sliding, contrary to what might seem intuitive. In fact, several feedbacks play out under the ice. For example, as meltwater input increases, water pressure under the ice increases, leading to enhanced basal lubrication and higher sliding velocity (Zwally et al., 2002). But with sustained meltwater input over a melt season, more efficient drainage channels can develop, decreasing the water pressure (Schoof, 2010). Characteristics of individual outlet glaciers such as bed topography, ice geometry, surface temperature, and other factors all play into the intricate choreography of the seasonal evolution of the subglacial drainage system and its influence on ice velocity.

In this paper, we describe the model SHaKTI (Subglacial Hydrology and Kinetic Transient Interactions), a model formulation that allows for flexible evolution of the subglacial drainage system configuration and flow regimes. The paper is structured as follows: in the next section, we provide a brief summary and review of historical and recent subglacial hydrology modeling progress to put our model in context. We then present the model's governing equations, the numerical framework, and illustrative simulations to demonstrate key model features and capabilities.

1.1 Subglacial hydrology modeling context

The first major efforts to quantitatively model subglacial hydrology began in the 1970s. Shreve (1972) described a system of arborescent subglacial channels, and Röthlisberger (1972) formulated equations for semi-circular channels melted into the base of the ice sheet, in a state of equilibrium between melt opening and creep closure. Nye (1973) expanded the work of Röthlisberger to consider channels incised into bedrock or subglacial sediments, and more fully developed the equations into models for explaining outburst floods (Nye, 1976). In a different approach, Weertman (1972) considered subglacial drainage through a water sheet of approximately uniform thickness. In the following decade, different plausible drainage configurations were also proposed, such as a system of "linked cavities", spaces that open behind bedrock bumps as a result of glacier sliding

Geosci. Model Dev. Discuss., https://doi.org/10.5194/gmd-2018-58
Manuscript under review for journal Geosci. Model Dev.
Discussion started: 27 March 2018

(Walder, 1986; Kamb, 1987). By the mid-1980s, it was recognized that the major components of subglacial hydrology could be classified as either efficient channels or less efficient distributed systems of linked cavities (often represented in continuum models as a sheet). While channels themselves emerge as a result of self-organized selective growth from a linked cavity system, a clear distinction between these two subsystems was established.

In the 1980s and 1990s, a handful of observational studies highlighted the influence of subglacial water pressure on glacier and ice sheet sliding (e.g., Iken, 1981; Iken and Bindschadler, 1986; Kamb, 1987; Murray and Clarke, 1995; Iken and Truffer, 1997), and modeling studies were undertaken considering diverse drainage schemes to understand subglacial hydrology. These included drainage through permeable till beneath a glacier (Shoemaker, 1986), channels incised into the bedrock or sediment (Walder and Fowler, 1994), and a zero-dimensional "box" model drawing an analogy to electrical circuits with lumped elements (Clarke, 1996).

Since 2000, a renewed surge of interest in subglacial hydrology has been sparked as mass loss increases from Greenland and sea level rise is increasingly perceived as an imminent reality, generating a flurry of new observations and modeling advances. Although the link between surface melt and ice sheet dynamics is still poorly understood (e.g., Clarke, 2005; Joughin et al., 2008), observations have reinforced the fact that surface meltwater significantly influences flow behavior in alpine glaciers and ice sheets (e.g., Mair et al., 2002; Zwally et al., 2002; Bartholomaus et al., 2008; Howat et al., 2008; Shepherd et al., 2009; Bartholomew et al., 2010; Hoffman et al., 2011; Sundal et al., 2011; Bartholomew et al., 2012; Meierbachtol et al., 2013; Andrews et al., 2014). Along with more detailed observations, several efforts were made in the early 2000s to accurately simulate subglacial hydrology. Some of these studies treated the subglacial system as a water sheet of uniform thickness (e.g., Flowers and Clarke, 2001; Flowers and Clarke, 2002; Johnson and Fastook, 2002; Creyts and Schoof, 2009; LeBrocq et al., 2009). Arnold and Sharp (2002) presented a model with both distributed and channel flow, but only one configuration could operate at a time. Kessler and Anderson (2004) introduced a model using discrete drainage pathways that could transition between distributed and channelized modes, and Flowers et al. (2004) used a combination of a distributed sheet in parallel with a network of efficient channels. Schoof (2010) developed a 2D network of discrete conduits that could behave like either channels or cavities, and found that with sufficiently large discharge an arborescent network of channel-like conduits would form, although the resulting geometry was highly dependent on the rectangular grid used. Hewitt (2011) developed a model that used a water sheet to represent evolving linked cavities averaged over a patch of bed (an effective porous medium), coupled to a single channel.

More recent studies tied together key elements of subglacial drainage to form more realistic 2D models. Hewitt (2013) introduced a linked-cavity continuum sheet integrated with a structured channel network. In that model, channels open by melt, while the distributed sheet opens only by sliding over bedrock bumps (neglecting opening by melt from dissipative heat). Melt in the channels is from dissipative heat only, while melt in the sheet is produced by geothermal flux and frictional heat from sliding. Werder et al. (2013) presented a model that involves water flow through a sheet (representative of averaged linked cavities) along with channels that are free to form along edges of the unstructured numerical mesh, exchanging water with the surrounding sheet. Bougamont et al. (2014) approached the problem in a different way, reproducing seasonal ice flow variability through the hydro-mechanical response of soft basal sediment in lieu of simulating the evolution of a subglacial

Geosci. Model Dev. Discuss., https://doi.org/10.5194/gmd-2018-58
Manuscript under review for journal Geosci. Model Dev.
Discussion started: 27 March 2018

Geoscientific Model Development Discussions
Open Access
EGU

drainage system. DeFleurian et al. (2014) employed a 2D dual-layer porous medium model to capture broad characteristics of subglacial drainage without resolving individual elements. Bueler and Pelt (2015) formulated equations for a 2D model that combines water stored in subglacial till with linked cavities. Hoffman et al. (2016) introduced a component to represent hydraulically isolated or "weakly connected" regions of the bed to help explain observations of high water pressure in late summer and fall.

1.2 Distinction between efficient channels and inefficient distributed drainage

A clear tradition has been established in the subglacial hydrology modeling literature of distinguishing between channelized (efficient) and distributed (inefficient) drainage systems or components. In most existing models, either only one of these forms is considered, or else different equations are applied to coupled "channel" or "sheet" components (even in models where channels are allowed to freely evolve within a sheet configuration, as in Werder et al., 2013). As a notable exception, Schoof (2010) examined the instability of conduits that could behave as either channels or linked cavities, and found that beyond a threshold effective pressure a channel-like conduit would become unstable, with the melt rate exceeding the closure rate, leading to further enlargement (this unstable growth may drive initiation of glacial floods). Hewitt (2011) asserted that the dissipation instability of a distributed sheet system is the process that spurs channelization, and used linear stability analysis to argue that this process has a runaway effect, resulting in exponential melt in an infinitesimally small area.

The artificial distinction of treating the distributed system and channels with different equations, however, remains questionable. Imposing a distinction that changes the governing physics under different flow regimes may not allow for the full array of drainage characteristics to arise, including isolated or "weakly connected" portions of the bed, as emphasized in Hoffman et al. (2016). In the model formulation described in this paper, a single set of governing equations is applied over the entire domain, with a spatially and temporally varying transmissivity that allows for representation of the wide transition between turbulent and laminar flow, and the geometry of each element is allowed to evolve accordingly to form flexible configurations. Our model does not aim to simulate every individual cavity or specific channel cross-section, but rather captures the homogenized effects of these elements on a discrete mesh. We include the dissipation term in the melt rate everywhere in the domain, and we are able to generate steady and stable transient drainage configurations that include obvious channel-like efficient drainage pathways. While our approach of treating the entire domain with the same equations departs from the precedent set by other subglacial hydrology models, it is satisfying to generate naturally arising drainage geometries that include distributed regions as well as channels, and even isolated portions of the bed or any other configuration that might emerge with realistic topography. This unified formulation could facilitate high-resolution exploration of the conditions under which different drainage system types may form and persist. With future application to actual outlet glaciers, this type of modeling may provide useful insights into the seasonal evolution of real subglacial drainage systems and their influence on mass loss from the Greenland ice sheet, with the potential for broader application to Antarctica and alpine glaciers.

Geosci. Model Dev. Discuss., https://doi.org/10.5194/gmd-2018-58
Manuscript under review for journal Geosci. Model Dev.
Discussion started: 27 March 2018

Geoscientific Model Development Discussions
Open Access
EGU

2 SHaKTI model description

This flexible subglacial hydrology model can handle transient meltwater inputs, both spatially distributed and localized, and allows the basal water flux and geometry to evolve according to these inputs to produce flow and drainage regimes across the spectrum from inefficient to efficient. Channels or channel locations are not prescribed a priori, but can arise and decay naturally as reflected in self-organized formation of connected paths of large gap height. The parallelized, finite element SHaKTI model is currently implemented as part of the Ice Sheet System Model (ISSM; Larour et al., 2012; http://issm.jpl.nasa.gov). Below, we present the equations involved in this formulation. The governing equations are similar to those used in Werder et al. (2013), with some key differences that enable application of the same set of equations everywhere in the domain.

2.1 Summary of model equations

The SHaKTI model is based upon governing equations that describe conservation of mass, evolution of the gap height, basal water flux (approximate momentum equation), and internal melt generation (approximate energy equation). This system of equations can be viewed as an approximation to a multi-dimensional generalization of the governing equations for glacial conduits described by Spring and Hutter (1981) and Clarke (2003). All variables used in the equations are summarized in Table 1, with constants and parameters summarized in Table 2.

Continuity equation (water mass balance):

$$\frac{\partial b}{\partial t} + \frac{\partial b_e}{\partial t} + \nabla \cdot \boldsymbol{q} = \frac{\dot{m}}{\rho_w} + i_{e \to b} \tag{1}$$

where b is subglacial gap height, b_e is the volume of water stored englacially per unit area of bed, $\boldsymbol{q}$ is basal water flux, $\dot{m}$ is basal melt rate, and $i_{e \to b}$ is the input rate of water from the englacial to subglacial system.

Basal gap dynamics (subglacial geometry):

$$\frac{\partial b}{\partial t} = \frac{\dot{m}}{\rho_i} + \beta u_b - A|p_i - p_w|^{n-1}(p_i - p_w)b \tag{2}$$

where A is the ice flow law parameter, n is the flow law exponent, p_i is the overburden pressure of ice, p_w is water pressure, β is a dimensionless parameter governing opening by sliding, and u_b is the magnitude of the sliding velocity. According to this equation, the subglacial gap height evolves with time by: opening by both melt and sliding over bumps on the bed, and closing due to ice creep.

Basal water flux (approximate momentum equation):

$$\boldsymbol{q} = \frac{-b^3 g}{12\nu(1 + \omega Re)} \nabla h \tag{3}$$

where g is gravitational acceleration, ν is kinematic viscosity of water, ω is a dimensionless parameter controlling the nonlinear transition from laminar to turbulent flow (for turbulent flow, $\omega Re >> 1$, the flux is proportional to the square root of the head gradient magnitude, whereas for $\omega Re << 1$, the flux is proportional to the head gradient magnitude), Re is the Reynolds number, and h is hydraulic head:

$$h = \frac{p_w}{\rho_w g} + z_b \tag{4}$$

Geosci. Model Dev. Discuss., https://doi.org/10.5194/gmd-2018-58
Manuscript under review for journal Geosci. Model Dev.
Discussion started: 27 March 2018

Geoscientific Model Development Discussions

where ρ_w is density of liquid water and z_b is bed elevation. The momentum equation is approximate in the sense that acceleration terms are neglected. Equation (3) is a key piece of our model formulation, in that it allows for a spatially and temporally variable hydraulic transmissivity in the system, and facilitates representation of both laminar and turbulent flow regimes, coexistence of laminar and turbulent flow in subregions, as well as flow that pertains to the wide transition between laminar and turbulent, where the linearity of laminar flow is not valid, but the square root dependence doesn't fully apply. This equation is based on flow equations for rock fractures and has been employed in that context previously (Zimmerman et al., 2004; Rajaram et al., 2009; Chaudhuri et al., 2013). Most existing subglacial hydrology models prescribe a hydraulic conductivity parameter and assume the flow to be turbulent everywhere.

Internal melt generation (energy balance at the bed):

$$\dot{m} = \frac{1}{L}(G + |\boldsymbol{u_b} \cdot \boldsymbol{\tau_b}| - \rho_w g \boldsymbol{q} \cdot \nabla h - c_t c_w \rho_w \boldsymbol{q} \cdot \nabla p_w) \tag{5}$$

where L is latent heat of fusion of water, G is geothermal flux, $\boldsymbol{u_b}$ is the ice basal velocity vector, $\boldsymbol{\tau_b}$ is the stress exerted by the bed onto the ice, c_t is the change of pressure melting point with temperature, and c_w is the heat capacity of water. Melt is therefore produced through a combination of geothermal flux, frictional heat due to sliding, and heat generated through internal dissipation (where mechanical energy is converted to thermal energy), minus the heat consumed due to changes in water pressure. We note that this form of the energy equation assumes that all heat produced is converted locally to melt and neglects transport of dissipative heat. We assume that the ice and liquid water are isothermal, consistently at the pressure melting point temperature. These assumptions may not be strictly valid under certain real conditions that may have interesting heat transfer implications, in which heat is advected downstream or meltwater enters a system of cold (below the pressure melting point) ice, but we leave these potential model extensions for future work.

Following Werder et al. (2013), the englacial storage volume is a function of water pressure:

$$b_e = e_v \frac{\rho_w g h - \rho_w g z_b}{\rho_w g} = e_v (h - z_b) \tag{6}$$

where e_v is the englacial void ratio (zero for no englacial storage).

Equations (1), (2), (3), and (5) are combined to form a parabolic, nonlinear partial differential equation (PDE) in terms of hydraulic head, h:

$$\nabla \cdot \left[\frac{-b^3 g}{12\nu(1+\omega Re)} \nabla h \right] + \frac{\partial e_v (h - z_b)}{\partial t} = \dot{m} \left[\frac{1}{\rho_w} - \frac{1}{\rho_i} \right] + A|p_i - p_w|^{n-1}(p_i - p_w)b - \beta u_b + i_{e \rightarrow b} \tag{7}$$

With no englacial storage ($e_v = 0$), Eq. (7) takes the form of an elliptic PDE.

Defining a hydraulic transmissivity tensor:

$$\boldsymbol{K} = \frac{b^3 g}{12\nu(1+\omega Re)} \mathbf{I} \tag{8}$$

Equation (7) can be written more compactly as:

$$\nabla \cdot (-\boldsymbol{K} \cdot \nabla h) + \frac{\partial e_v (h - z_b)}{\partial t} = \dot{m} \left(\frac{1}{\rho_w} - \frac{1}{\rho_i} \right) + A|p_i - p_w|^{n-1}(p_i - p_w)b - \beta u_b + i_{e \rightarrow b} \tag{9}$$

Geosci. Model Dev. Discuss., https://doi.org/10.5194/gmd-2018-58
Manuscript under review for journal Geosci. Model Dev.
Discussion started: 27 March 2018

Geoscientific Model Development Discussions

Although we employ an isotropic representation of the hydraulic transmissivity tensor in Eq. (8), our model formulation can be readily generalized to incorporate anisotropy. The source terms on the right-hand side of the equation depend on h (see Eq. 4), so there are nonlinearities to deal with in solving for the head distribution.

2.2 Boundary conditions

Boundary conditions can be applied as either prescribed head (Dirichlet) conditions or as flux (Neumann) conditions. We typically apply a Dirichlet boundary condition of atmospheric pressure at the edge of the ice sheet, and Neumann boundary conditions (no flux or prescribed flux, which can be constant or time-varying) on the other boundaries of the subglacial drainage domain.

In our current formulation, there is no lower limit imposed on the water pressure; this means that unphysical negative pressures can be calculated in the presence of steep bed slopes, as in Werder et al. (2013). While suction and cavitation may occur in these situations, the flow most likely transitions to free-surface flow with the subglacial gap partially filled by air or water vapor. At high water pressure, we restrict the value to not exceed the ice overburden pressure, which would manifest as uplift of the ice or hydrofracturing at the bed. These extreme "underpressure" and "overpressure" regimes are important situations that have been considered carefully in other studies (e.g., Tsai and Rice, 2010; Hewitt et al., 2012; Schoof et al., 2012;), and will be addressed in future model developments.

2.3 Computational strategy and implementation in the Ice Sheet System Model (ISSM)

Within each time step, the nonlinear Eq. (9) is solved using an implicit Euler-Backward discretization and Picard iteration to obtain the head (h) field. From h, we calculate p_w, $\boldsymbol{q}$, Re, and $\dot{m}$, to be used in the subsequent iteration (in each iteration, p_w, $\boldsymbol{q}$, Re, and $\dot{m}$ are lagged from the previous iteration). Once the Picard iteration has successfully converged to a solution for h, the gap height geometry is then updated explicitly based on basal gap dynamics using Eq. (2) to advance to the next time step. A schematic of this numerical procedure is presented in Fig. 1.

SHaKTI is implemented within ISSM, an open source ice dynamics model for Greenland and Antarctica developed by NASA's Jet Propulsion Laboratory and University of California at Irvine (Larour et al., 2012; http://issm.jpl.nasa.gov). ISSM uses finite element methods and parallel computing technologies, and includes sophisticated data assimilation and sensitivity analysis tools, to support numerous capabilities for ice sheet modeling applications on a variety of scales. The SHaKTI hydrology model solves the equations presented above in a parallel architecture using linear finite elements (i.e. P1 triangular Lagrange finite elements). The source code is written in C++ and we rely on data structures and solvers provided by the Portable, Extensible Toolkit for Scientific Computation (PETSc, http://www.mcs.anl.gov/petsc). The user interface in MATLAB is the same as for other solutions implemented in ISSM, designed to facilitate model set up and post processing (see Documentation, https://issm.jpl.nasa.gov/documentation/hydrologyshakti/). The nonlinear iteration is performed to solve Eq. (9) for hydraulic head using the direct linear solver MUMPS in PETSc, but other solvers provided by PETSc could be easily tested in future work.

Geosci. Model Dev. Discuss., https://doi.org/10.5194/gmd-2018-58
Manuscript under review for journal Geosci. Model Dev.
Discussion started: 27 March 2018

Model inputs include spatial fields of bed elevation, ice surface elevation, initial hydraulic head, initial basal gap height, ice sliding velocity, basal friction coefficient, typical bed bump height and spacing, englacial input to the bed (which can be constant or time-varying, and can be spatially distributed or located at discrete points to represent moulin input), and appropriate boundary conditions. Parameters that can either be specified or rely on a default value are geothermal flux, the ice flow law parameter and exponent, and the englacial storage coefficient.

Model outputs include spatiotemporal fields of hydraulic head, effective pressure, subglacial gap height (the effective geometry representative of an entire element), depth-integrated water flux, and "degree of channelization" (the ratio of opening by melt in each element to the total rate of opening in that element by both melt and sliding). Head and effective pressure are calculated at each vertex on the mesh; gap height, water flux, and degree of channelization are constant over an entire element (since these quantities are based on the head gradient). All model outputs are readily available in matrix form to be analyzed and processed in a variety of ways, or visualized through contour plots, time series plots, and movie animations. ISSM includes several custom plotting scripts, and data can also be visualized or analyzed via any standard MATLAB tools. Instructions for setting up, running a simulation, and plotting outputs can be found in the SHaKTI model documentation (https://issm.jpl.nasa.gov/documentation/hydrologyshakti/) and in an example tutorial (https://issm.jpl.nasa.gov/documentation/tutorials/shakti/).

3 Application

To demonstrate the capabilities of SHaKTI, here we present illustrative simulations that highlight some of its features.

3.1 Channel formation from discrete moulin input

In this first example, we consider a 1 km square, 500 m thick tilted ice slab with surface and bed slope of 0.02 along the x direction. Steady input of 4 $m^3\ s^{-1}$ is prescribed at a single moulin at the center of the square (x=500 m, y=500 m). Water pressure at the outflow (left edge of the domain, x=0) is set to atmospheric pressure, with zero flux boundary conditions at the other three sides of the domain. All other constants and parameters are as described in Table 2. When run to a steady configuration with a time step of 900 s, an efficient drainage "channel" emerges from the moulin to the outflow, with higher effective pressure (i.e. lower head and water pressure), larger gap height, and higher basal flux than its surroundings (Fig. 2). Scripts for running this example are included as a tutorial in ISSM (https://issm.jpl.nasa.gov/documentation/tutorials/shakti/), and can serve as a template for more sophisticated simulations.

3.2 Channelization with multiple moulins and mesh refinement

For the next example, we consider a rectangular domain 10 km long and 2 km wide, with a flat bed ($z_b = 0$ everywhere) and parabolic surface profile as shown in Fig. 3a. Ten moulins are located at arbitrarily chosen locations in the domain (shown in Fig. 3c), each with a steady input of 10 $m^3\ s^{-1}$. The resulting steady head and gap height distributions (Figs. 3b and 3c) show a clear channelization structure. Rather than each moulin forming a unique channel to the outflow, the moulin inputs influence

Geosci. Model Dev. Discuss., https://doi.org/10.5194/gmd-2018-58
Manuscript under review for journal Geosci. Model Dev.
Discussion started: 27 March 2018

each other, warping the pressure field and forming efficient pathways that combine downstream. For this specific arrangement of moulin inputs, a single principal drainage channel emerges. The unique drainage configuration that evolves is affected by many factors, including bed topography, ice thickness, sliding velocity, meltwater input location, and input intensity. The exact configuration of self-organizing channels also depends to some extent on the mesh. Our unstructured mesh reduces bias in channel direction compared to a structured mesh, but the orientation of elements does still affect the resulting geometry. The different cases shown in Fig. 3 provide a qualitative view of dependence on mesh size: the effective gap height across each element obviously varies, but the head field (and corresponding effective pressure that drives ice sliding velocity) is quite similar. Quantitative plots of head difference between the different meshes are included in the supplementary material.

3.3 Seasonal variation and distributed meltwater input

Next we consider a transient example involving a seasonal input cycle of meltwater, with input distributed uniformly across a rectangular domain 4 km long and 8 km wide. The bed is flat ($z_b = 0$ everywhere). The ice surface follows a parabolic profile, with ice thickness ranging from 550 m at x=0 to 700 m at x=4 km, and is uniform across the y direction. We begin with an initial subglacial gap height of 0.01 m, perturbed with random variations drawn from a normal distribution with standard deviation of 1%. The purpose of these random variations in the initial gap height is to serve as triggers for potential instability and channelization, which is an important phenomenon in subglacial hydrologic systems (Walder, 1986; Kamb, 1987; Schoof, 2010; Hewitt et al., 2011). Even in nature, the gap height is unlikely to be uniform and the ubiquitous irregular variations in the gap height and bedrock surface will act as natural perturbations to initiate instabilities and channelization. As the ice slides over bedrock, abrasion processes may also serve to generate irregularities. In the literature on the self-organized formation of dissolution channels in rock fractures (e.g. Cheung and Rajaram, 2002; Scymzak and Ladd, 2006; Rajaram et al., 2009), it has been established that under conditions that lead to self-organized channel formation, the specific nature of the initial random variations do not influence the structure and spacing of the channels; rather they serve as a trigger for the initiation of channels. In unstructured meshes, it is also possible for mesh-related asymmetries to introduce perturbations that can serve as triggers for this instability. In stable regimes, however, the same perturbations will not produce channelization. The model is first run with steady low distributed input in a spin-up stage. After a steady configuration is achieved, a seasonal cycle of meltwater input variation is imposed. Seasonal meltwater input in m a^{-1} is approximated by a cosine function between 0.4-0.7 (days 146 and 255) of each year:

$$i_{e\rightarrow b} = -492.75 \times \cos(2\pi/0.3(t-0.4)) + 493.75 \tag{10}$$

This yields a maximum meltwater input at the peak of the summer of 986 m a^{-1}, with a winter minimum of 1 m a^{-1}, and annual mean input of 149 m a^{-1}. The peak melt input corresponds to approximately 1,000 m^3 s^{-1} for the entire domain. Figure 4a shows time series plots of the seasonal input forcing over one full annual cycle, with the corresponding minimum, mean, and maximum gap height (Fig. 4b) and head (Fig. 4c). Snapshots of the gap height and head distributions at intervals through the annual cycle are shown in Fig. 5, and an animation of this simulation is included in the supplementary material.

Geosci. Model Dev. Discuss., https://doi.org/10.5194/gmd-2018-58
Manuscript under review for journal Geosci. Model Dev.
Discussion started: 27 March 2018

As melt increases, the maximum gap height increases, corresponding to growth of the subglacial system and emergence of self-organized efficient channels. The maximum gap height increases with increasing meltwater input until the peak of the melt season, then decreases simultaneously as melt input decreases (note that we do not include the storage term in this simulation). The hydraulic head initially increases with increased input (meaning an increase in subglacial water pressure as additional water is added to the system), then decreases as efficient low-pressure channels form, then increases again as melt starts to decrease and the channels collapse. Ice sheet sliding velocity generally increases with increased water pressure (i.e. lower effective pressure) and decreases with lower water pressure. The sequence of hydraulic head or basal water pressure variation seen here would result in a late summer decline in sliding velocity, after which the sliding velocity would increase again. Subsequently, as melt input decreases to the winter minimum, the hydraulic head decreases to low values. As shown in Fig. 5, for the early and late parts of the year, the system essentially behaves as a one-dimensional system, because the melt inputs are not large enough to take the system into an unstable regime where channelization can occur. During the melt season, when inputs increase substantially, self-organized, regularly spaced channels emerge, seen in Fig. 5 as having lower heads than their immediate surroundings in the y direction. These channels collapse and disappear entirely as the meltwater input drops off and returns to the winter minimum. The simulation results shown here establish the ability of our modeling framework to represent both stable regimes, where the subglacial system takes on a relatively smooth quasi-one-dimensional configuration, and unstable regimes with self-organized channels when high meltwater inputs and discharge trigger the transition to channelization. The transition to a channelized state in subglacial hydrologic systems has been described elegantly in previous work (Walder, 1986; Kamb, 1987; Schoof, 2010; Hewitt et al., 2011).

4 Discussion

The flexible geometry and flow regimes of the SHaKTI model allow for various drainage configurations to arise naturally, without needing to impose potential channel locations or separate the domain into subdomains with distinct governing equations. We conserve mass and energy in all parts of the domain, in contrast to several existing models that neglect the role of melt opening in distributed drainage systems. Previous studies found that with similar equations, including the melt term in a distributed system leads to an inevitable instability and runaway growth, which has been acknowledged as the spark that initiates channelization (Schoof, 2010; Hewitt, 2011). In our formulation, however, even with the melt term included, we are able to achieve stable configurations of subglacial geometry, basal water flux, and pressure fields with steady and transient input forcing. Efficient drainage pathways with lower water pressure than their surroundings form from moulin inputs (Figs. 2 and 3) as well as self-organized configurations with high distributed melt input (Fig. 5). A feature of our formulation that contributes to this controlled behavior is the way we calculate the basal water flux (approximate momentum equation, Eq. 3), which allows for a transient, spatially variable transmissivity that transitions naturally between laminar and turbulent flow regimes locally, while allowing both types of flow regime to coexist in the model domain, as well as flow that exhibits attributes along the wide transition between laminar and turbulent flow. Indeed, if we force the flux to be turbulent everywhere (by using a large value for ω in Eq. 3, so that $\omega Re >> 1$ always), the model produces runaway growth of the gap height and melt for the same

model problems in which bounded growth results when we allow for laminar, transitional, and turbulent flow. The concept of laminar-turbulent transition is well established in hydraulics and fluid mechanics, and our representation of the nonlinear flux-gradient relationship (Eq. 3) is consistent with this concept and is also consistent with experimental studies of Zimmerman et al. (2004).

The transient example in the preceding section clearly illustrates one possible pattern of seasonal evolution of the subglacial drainage system, where efficient pathways emerge with increased melt and collapse to a purely distributed/sheet system again in the winter. The higher water pressure during the melt season corresponds to increased sliding velocity, with a decrease in late summer with well established channels, followed by an increase as the channel system initiates its shutdown, and a decrease as melt returns to the background winter rate. This seasonal pattern is reminiscent of observations of some Greenland outlet glaciers (Moon et al., 2014), and supports the notion that subglacial hydrology may indeed play a key role in shaping the seasonal velocity behavior of some glaciers. In future work on real topography, we aim to produce other velocity signatures, such as those that experience an annual minimum velocity in the late melt season, which is thought to be a result of highly efficient channel development (Moon et al., 2014) or those with high winter sliding velocities, which may be indicative of hydraulically isolated or poorly connected regions of the bed (Hoffman et al., 2016).

We calculate basal gap height over each element, which means that the geometry is dependent on mesh size. It is not our aim to necessarily capture each individual cavity or channel cross-section, but rather to obtain the effective geometry over each element and its effect on the pressure field, which has an important influence on ice sheet sliding velocity. With very large elements, obviously the effects of efficient drainage channels may be smoothed out. For large-scale simulations, a variable mesh may be used with coarser resolution in the ice sheet interior away from the margins, with finer resolution at lower elevations where the bulk of meltwater is produced and enters the subglacial system (where efficient channel networks are likely to form).

5 Conclusions

In this paper, we presented the SHaKTI model formulation with simple illustrative simulations to highlight some of the model features under different conditions. The model is similar to previous subglacial hydrology models, but employs a single set of "unified" governing equations over the entire domain, without imposing a distinction between channelized or distributed systems. The geometry is free to evolve; efficient, low-pressure drainage channels can and do form as the subglacial system sorts itself out and facilitates transitions between different flow regimes. We find that with high meltwater input (via moulins or distributed input), self-organized channels emerge with higher effective pressure (i.e. lower water pressure) than their surrounding areas. As meltwater input decreases, these efficient drainage systems collapse and disappear.

To understand the overall mass balance and behavior of the Greenland ice sheet, it is crucial to understand the different seasonal velocity patterns observed on its outlet glaciers, and the corresponding enigmatic drainage systems hidden beneath the ice. Combined with advances in remote and field-based observations, and modeling of other processes involved in the hydrologic cycle of the Greenland ice sheet (such as surface mass balance, meltwater percolation and retention, and englacial transport of water), this subglacial hydrology model formulation may help close a gap in ice dynamics models to inform

predictions of future mass loss and sea level rise. Forthcoming work will focus on application of the SHaKTI model to real Greenland outlet glaciers and coupling the model to an ice dynamics model (ISSM, into which SHaKTI is already built).

Code availability. The SHaKTI model is freely available as part of the open source Ice Sheet System Model (ISSM), which is hosted in a subversion repository. https://issm.jpl.nasa.gov/download/

Author contributions. HR and AS formulated the model equations. AS wrote the stand-alone versions of the finite volume and finite element models. MM built the parallel model into ISSM and assisted AS with further model development. AS performed simulations and compiled the manuscript with contributions from HR and MM.

Competing interests. The authors declare that they have no conflicts of interest.

Acknowledgements. This work was primarily supported by a NASA Earth and Space Science Fellowship award (NNX14AL24H) to AS. A version of this model was originally presented in a 2010 proposal by HR and Robert Anderson. We thank Robert Anderson for his continued encouragement. Special thanks to Matthew Hoffman for many helpful conversations about subglacial hydrology modeling, to Basile DeFleurian and Mauro Werder for including our model in the Subglacial Hydrology Model Intercomparison Project (SHMIP, https://shmip.bitbucket.io/) and providing useful insights along the way, and to Eric Larour for his initial enthusiasm that facilitated our collaboration with ISSM.

Geosci. Model Dev. Discuss., https://doi.org/10.5194/gmd-2018-58
Manuscript under review for journal Geosci. Model Dev.
Discussion started: 27 March 2018

References

Andresen, C.S., F. Straneo, M.H. Ribergaard, A.A. Bjork, T.J. Andersen, A. Kujipers, N. Norgaard-Pedersen, K.H. Kjaer, K. Weckstrom, and A. Alhstrom (2011), Enhanced calving of Helheim Glacier over the last century forced by the ocean and atmosphere, Nature Geosci.

Andrews, L. C., Catania, G. A., Hoffman, M. J., Gulley, J. D., Lüthi, M. P., Ryser, C., Hawley, R.L., and Neumann, T. A. (2014). Direct observations of evolving subglacial drainage beneath the Greenland Ice Sheet. Nature, 514(7520), 80-83.

Arnold, N., and M. Sharp (2002), Flow variability in the Scandinavian ice sheet: Modelling the coupling between ice sheet flow and hydrology, Quat. Sci. Rev., 21(4–6), 485–502.

Bartholomaus, T. C., Anderson, R. S., and Anderson, S. P. (2008). Response of glacier basal motion to transient water storage. Nature Geoscience, 1(1), 33-37.

Bartholomew, I., Nienow, P., Mair, D., Hubbard, A., King, M. A., and Sole, A. (2010). Seasonal evolution of subglacial drainage and acceleration in a Greenland outlet glacier. Nature Geoscience, 3(6), 408-411.

Bartholomew, I., P. Nienow, A. Sole, D.W.F. Mair, T. Cowton, and M.A. King (2012), Short-term variability in Greenland Ice Sheet motion forced by time-varying meltwater inputs: Implications for the relationship between subglacial drainage system behavior and ice velocity, J. Geophys. Res.

Bell, R. E. (2008), The role of subglacial water in ice-sheet mass balance, Nat. Geosci., 1(5), 297–304, doi:10.1038/ngeo186.

Bougamont, M., Christoffersen, P., A L, H., Fitzpatrick, A. A., Doyle, S. H., and Carter, S. P. (2014). Sensitive response of the Greenland Ice Sheet to surface melt drainage over a soft bed. Nature communications, 5.

Bueler, E., and Pelt, W. V. (2015). Mass-conserving subglacial hydrology in the Parallel Ice Sheet Model version 0.6. Geoscientific Model Development, 8(6), 1613-1635.

Chaudhuri, A., Rajaram, H. and Viswanathan, H. (2013). Early stage hypogene karstification in a mountain hydrologic system: A coupled thermohydrochemical model incorporating buoyant convection. Water Resources Research, 49(9), pp.5880-5899.

Cheung, W., and Rajaram, H. (2002). Dissolution finger growth in variable aperture fractures: Role of the tip region flow field. Geophysical research letters, 29(22).

Clarke, G. C. K. (1996), Lumped-elements analysis of subglacial hydraulic circuits, J. Geophys. Res., 101(B8), 17,547–17,559.

Clarke, G. K. (2003). Hydraulics of subglacial outburst floods: new insights from the Spring-Hutter formulation. Journal of Glaciology, 49(165), 299-313.

Clarke, G. K. (2005). Subglacial processes. Annu. Rev. Earth Planet. Sci., 33, 247-276.

Colgan, W., H. Rajaram, R.S. Anderson, K. Steffen, J.H. Zwally, T. Phillips, and W. Abdalati (2011), The annual glaciohydroogy cycle in the ablation zone of the Greenland ice sheet: Part 2. Observed and modeled ice flow, J. Glaciol.

Cowton, T., P. Nienow, A. Sole, J. Wadham, G. Lis, I. Bartholomew, D. Mair, and D. Chandler (2013), Evolution of drainage system morphology at a land-terminating Greenland outlet glacier, J. Geophys. Res. Earth Surf.

Das, S. B., Joughin, I., Behn, M. D., Howat, I. M., King, M. A., Lizarralde, D., and Bhatia, M. P. (2008). Fracture propagation to the base of the Greenland Ice Sheet during supraglacial lake drainage. Science, 320(5877), 778-781.

DeConto, R. M., and Pollard, D. (2016). Contribution of Antarctica to past and future sea-level rise. Nature, 531(7596), 591-597.

Doyle, S.H., Hubbard, A., Van De Wal, R.S., van As, D., Scharrer, K., Meierbachtol, T.W., Smeets, P.C., Harper, J.T., Johansson, E., Mottram, R.H. and Mikkelsen, A.B. (2015). Amplified melt and flow of the Greenland ice sheet driven by late-summer cyclonic rainfall. Nature Geoscience, 8(8), pp.647-653.

Flowers, G. E., and G. K. C. Clarke (2002), A multicomponent coupled model of glacier hydrology - 1. Theory and synthetic examples, J. Geophys. Res., 107(B11), 2287, doi:10.1029/2001JB001122.

Forster, R. R., van den Broeke, M. R., Miège, C., Burgess, E. W., van Angelen, J. H., Lenaerts, J. T., and Leuschen, C. (2014). Extensive liquid meltwater storage in firn within the Greenland ice sheet. Nature Geoscience, 7(2), 95-98.

Hewitt, I. J. (2011), Modelling distributed and channelized subglacial drainage: The spacing of channels, J. Glaciol, 57(202), 302–314.

Hewitt, I. J., C. Schoof, and M. A. Werder (2012), Flotation and free surface flow in a model for subglacial drainage. Part II: Channel flow, J. Fluid Mech., 702, 157–187, doi:10.1017/jfm.2012.166.

Hewitt, I. J. (2013), Seasonal changes in ice sheet motion due to melt water lubrication, Earth Planet. Sci. Lett., 371, 16–25, doi:10.1016/j.epsl.2013.04.022.

Hoffman, M. J., G. A. Catania, T. A. Neumann, L. C. Andrews, and J. A. Rumrill (2011), Links between acceleration, melting, and supraglacial lake drainage of the western Greenland Ice Sheet, J. Geophys. Res., 116, F04035, doi:10.1029/2010JF001934.

Hoffman, M., and Price, S. (2014). Feedbacks between coupled subglacial hydrology and glacier dynamics. Journal of Geophysical Research: Earth Surface, 119(3), 414-436.

Hoffman, M.J., Andrews, L.C., Price, S.A., Catania, G.A., Neumann, T.A., Lüthi, M.P., Gulley, J., Ryser, C., Hawley, R.L. and Morriss, B. (2016). Greenland subglacial drainage evolution regulated by weakly connected regions of the bed. Nature communications, 7, p.13903.

Howat, I. M., S. Tulaczyk, E. Waddington, and H. Björnsson (2008), Dynamic controls on glacier basal motion inferred from surface ice motion, J. Geophys. Res., 113(F3), F03015, doi:10.1029/2007JF000925.

Howat, I. M., A. Negrete, and B. E. Smith (2014), The Greenland Ice Mapping Project (GIMP) land classification and surface elevation data sets, Cryosphere, 8(4), 1509–1518, doi:10.5194/tc-8-1509-2014.

Iken, A. (1981). The effect of the subglacial water pressure on the sliding velocity of a glacier in an idealized numerical model. Journal of Glaciology, 27(97), 407-421.

Iken, A., and Bindschadler, R. A. (1986). Combined measurements of subglacial water pressure and surface velocity of Findelengletscher, Switzerland: conclusions about drainage system and sliding mechanism. Journal of Glaciology, 32(110), 101-119.

Iken, A., and Truffe, M. (1997). The relationship between subglacial water pressure and velocity of Findelengletscher, Switzerland, during its advance and retreat. Journal of Glaciology, 43(144), 328-338.

IPCC (2013), Climate Change 2013: The Physical Science Basis. Contribution of Working Group 1 to the Fifth Assessment Report of the Intergovernmental Panel on Climate Change [Stocker, T.F., D. Qin, G.-K. Plattner, S.K. Allen, J. Boschung, A. Nauels, Y. Xia, V. Bex and P.M. Midgley (eds.)], Cambridge University Press, Cambridge, United Kingdom and New York, NY, USA, 1535 pp.

Johnson, J., and J. L. Fastook (2002), Northern Hemisphere glaciation and its sensitivity to basal melt water, Quat. Int., 95, 65–74.

Joughin, I., Das, S. B., King, M. A., Smith, B. E., Howat, I. M., and Moon, T. (2008). Seasonal speedup along the western flank of the Greenland Ice Sheet. Science, 320(5877), 781-783.

Joughin, I., Smith, B. E., Howat, I. M., Scambos, T., and Moon, T. (2010). Greenland flow variability from ice-sheet-wide velocity mapping. Journal of Glaciology, 56(197), 415-430.

Joughin, I., Smith, B. E., and Medley, B. (2014). Marine ice sheet collapse potentially under way for the Thwaites Glacier Basin, West Antarctica. Science, 344(6185), 735-738.

Kamb, B. (1987). Glacier surge mechanism based on linked cavity configuration of the basal water conduit system. Journal of Geophysical Research: Solid Earth, 92(B9), 9083-9100.

Larour, E., H. Seroussi, M. Morlighem, and E. Rignot. Continental scale, high order, high spatial resolution, ice sheet modeling using the Ice Sheet System Model (ISSM) (2012). J. Geophys. Res., 117(F01022):1–20

Le Brocq, A., A. Payne, M. Siegert, and R. Alley (2009), A sub- glacial water-flow model for West Antarctica, J. Glaciol., 55(193), 879–888.

Lindbäck, K., Pettersson, R., Doyle, S.H., Helanow, C., Jansson, P., Kristensen, S.S., Stenseng, L., Forsberg, R. and Hubbard, A.L. (2014). High-resolution ice thickness and bed topography of a land-terminating section of the Greenland Ice Sheet. Earth System Science Data, 6(2), pp.331-338.

Lindbäck, K., Pettersson, R., Hubbard, A.L., Doyle, S.H., As, D., Mikkelsen, A.B. and Fitzpatrick, A.A. (2015). Subglacial water drainage, storage, and piracy beneath the Greenland ice sheet. Geophysical Research Letters, 42(18), pp.7606-7614.

Lipscomb, W., R. Bindschadler, S. Price, E. Bueler, J. Johnson, and D. Holland (2009), A community ice sheet model for sea level prediction, Eos, Trans. AGU, 90(3), 23, doi:10.1029/2009EO030004.

Little, C. M., et al. (2007), Toward a new generation of ice sheet models, Eos, Trans. AGU, 88(52), 578–579, doi:10.1029/2007EO520002.

Mair, D., Nienow, P., Sharp, M., Wohlleben, T., and Willis, I. (2002). Influence of subglacial drainage system evolution on glacier surface motion: Haut Glacier d'Arolla, Switzerland. Journal of Geophysical Research: Solid Earth, 107(B8).

McFadden, E.M., I.M. Howat, I. Joughin, B.E. Smith, and Y. Ahn (2011), Changes in the dynamics of marine terminating outlet glaciers in west Greenland(2000-2009) J.Geophys.Res.

Meierbachtol, T., J. Harper, and N. Humphrey (2013), Basal drainage system response to increasing surface melt on the Greenland ice sheet, Science

Meierbachtol, T.W., Harper, J.T., Humphrey, N.F. and Wright, P.J. (2016). Mechanical forcing of water pressure in a hydraulically isolated reach beneath Western Greenland's ablation zone. Annals of Glaciology, pp.1-9.

Moon, T., Joughin, I., Smith, B., Broeke, M. R., Berg, W. J., Noël, B., and Usher, M. (2014). Distinct patterns of seasonal Greenland glacier velocity. Geophysical research letters, 41(20), 7209-7216.

Morlighem, M., Rignot, E., Mouginot, J., Wu, X., Seroussi, H., Larour, E., and Paden, J. (2013). High-resolution bed topography mapping of Russell Glacier, Greenland, inferred from Operation IceBridge data. Journal of Glaciology, 59(218), 1015-1023.

Murray, T., and Clarke, G. K. (1995). Black box modeling of the subglacial water system. Journal of Geophysical Research: Solid Earth, 100(B6).

Nick, F.M., A. Vieli, I.M. Howat, and I. Joughin (2009), Large-scale changes in Greenland outlet glacier dynamics triggered at the terminus, Nature Geoscience.

Nye, J. F. (1973), Water at the bed of a glacier, in Proceedings of the Cambridge Symposium 1969, pp. 189–194, IASH, nr. 95.

Nienow, P. W., Sole, A. J., Slater, D. A., and Cowton, T. R. (2017). Recent Advances in Our Understanding of the Role of Meltwater in the Greenland Ice Sheet System. Current Climate Change Reports, 1-15.

Nye, J. F. (1976). Water flow in glaciers: jökulhlaups, tunnels and veins. Journal of Glaciology, 17(76), 181-207.

Pimentel, S., G. E. Flowers, and C. G. Schoof (2010), A hydrologically coupled higher-order flow-band model of ice dynamics with a Coulomb friction sliding law, J. Geophys. Res., 115(F4), F04023, doi:10.1029/2009JF001621.

Price, S., G. Flowers, and C. Schoof (2011), Improving hydrology in land ice models, Eos Trans. AGU, 92(19), 164.

Rajaram, H., Cheung, W. and Chaudhuri, A. (2009). Natural analogs for improved understanding of coupled processes in engineered earth systems: examples from karst system evolution. Current Science, pp.1162-1176.

Rennermalm, A., S. Moustafa, J. Mioduszewski, V. Chu, R. Forster, B. Hagedorn, J. Harper, T. Mote, D. Robinson, C. Shuman, L. Smith, and M. Tedesco (2013), Understanding Greenland ice sheet hydrology using an integrated multi-scale approach, Environmental Res. Lett.

Rignot, E., M. Koppes, and I. Velicogna (2010), Rapid subaqueous melting of the calving faces of West Greenland glaciers, Nature Geoscience

Röthlisberger, H. (1972). Water pressure in intra-and subglacial channels. Journal of Glaciology, 11(62), 177-203.

Schoof, C. (2010), Ice-sheet acceleration driven by melt supply variability, Nature, 468(7325), 803–806.

Schoof, C., I. J. Hewitt, and M. A. Werder (2012), Flotation and open water flow in a model for subglacial drainage. Part I: Linked cavities, J. Fluid Mech., 702, 126–156, doi:10.1017/ jfm.2012.165.

Shannon, S. R., et al. (2013), Enhanced basal lubrication and the contribution of the Greenland ice sheet to future sea-level rise, PNAS, 35(110), 14,156–14,161.

Shepherd, A., A. Hubbard, P. Nienow, M. King, M. McMillan, and I. Joughin (2009), Greenland ice sheet motion coupled with daily melting in late summer, Geophys. Res. Lett.

Shepherd, A., Ivins, E. R., Geruo, A., Barletta, V. R., Bentley, M. J., Bettadpur, S., and Horwath, M. (2012). A reconciled estimate of ice-sheet mass balance. Science, 338(6111), 1183-1189.

Shoemaker, E. M. (1986), Subglacial hydrology for an ice sheet resting on a deformable aquifer, J. Glaciol., 32(110), 20–30.

Shreve, R. L. (1972). Movement of water in glaciers. Journal of Glaciology, 11(62), 205-214.

Smith, L. C., Chu, V. W., Yang, K., Gleason, C. J., Pitcher, L. H., Rennermalm, A. K., and Tedesco, M. (2015). Efficient meltwater drainage through supraglacial streams and rivers on the southwest Greenland ice sheet. Proceedings of the National Academy of Sciences, 112(4), 1001-1006.

Spring, U., and Hutter, K. (1981). Numerical studies of jökulhlaups. Cold Regions Science and Technology, 4(3), 227-244.

Sundal, A.V., A. Shepherd, P. Nienow, E. Hanna, S. Palmer, and P. Huybrecths (2011), Melt-induced speed-up of Greenland ice sheet offset by efficient subglacial drainage, Nature

Vaughan, D.G., J.C. Comiso, I. Allison, J. Carrasco, G. Kaser, R. Kwok, P. Mote, T. Murray, F. Paul, J. Ren, E. Rignot, O. Solomina, K. Steffen, and T. Zhang (2013), Observations: Cryosphere. In: Climate Change 2013: The Physical Science Basis. Contribution of Working Group I to the Fifth Assessment Report of the Intergovernmental Panel on Climate Change.

Walder, J. S. (1986). Hydraulics of subglacial cavities. Journal of Glaciology, 32(112), 439-445.

Walder, J. S., and A. Fowler (1994), Channelized subglacial drainage over a deformable bed, J. Glaciol., 40(134), 3–15.

Weertman, J. (1972). General theory of water flow at the base of a glacier or ice sheet. Reviews of Geophysics, 10(1), 287-333.

Werder, M. A., Hewitt, I. J., Schoof, C. G., and Flowers, G. E. (2013). Modeling channelized and distributed subglacial drainage in two dimensions. Journal of Geophysical Research: Earth Surface, 118(4), 2140-2158.

Wright, P.J., Harper, J.T., Humphrey, N.F. and Meierbachtol, T.W. (2016). Measured basal water pressure variability of the western Greenland Ice Sheet: Implications for hydraulic potential. Journal of Geophysical Research: Earth Surface.

Zimmerman, R.W., Al-Yaarubi, A., Pain, C.C. and Grattoni, C.A. (2004). Non-linear regimes of fluid flow in rock fractures. International Journal of Rock Mechanics and Mining Sciences, 41, pp.163-169.

Zwally, H.J., W. Abdalati, T. Herring, K. Larson, J. Saba, K. Steffen (2002), Surface melt- induced acceleration of Greenland ice-sheet flow, Science

Geosci. Model Dev. Discuss., https://doi.org/10.5194/gmd-2018-58
Manuscript under review for journal Geosci. Model Dev.
Discussion started: 27 March 2018

Geoscientific Model Development Discussions

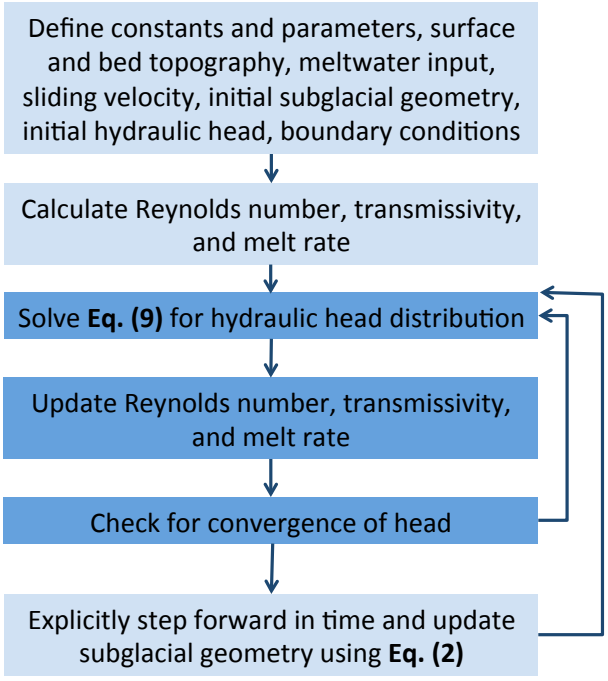

Figure 1. Schematic of computational procedure used to solve the model equations

Geosci. Model Dev. Discuss., https://doi.org/10.5194/gmd-2018-58
Manuscript under review for journal Geosci. Model Dev.
Discussion started: 27 March 2018

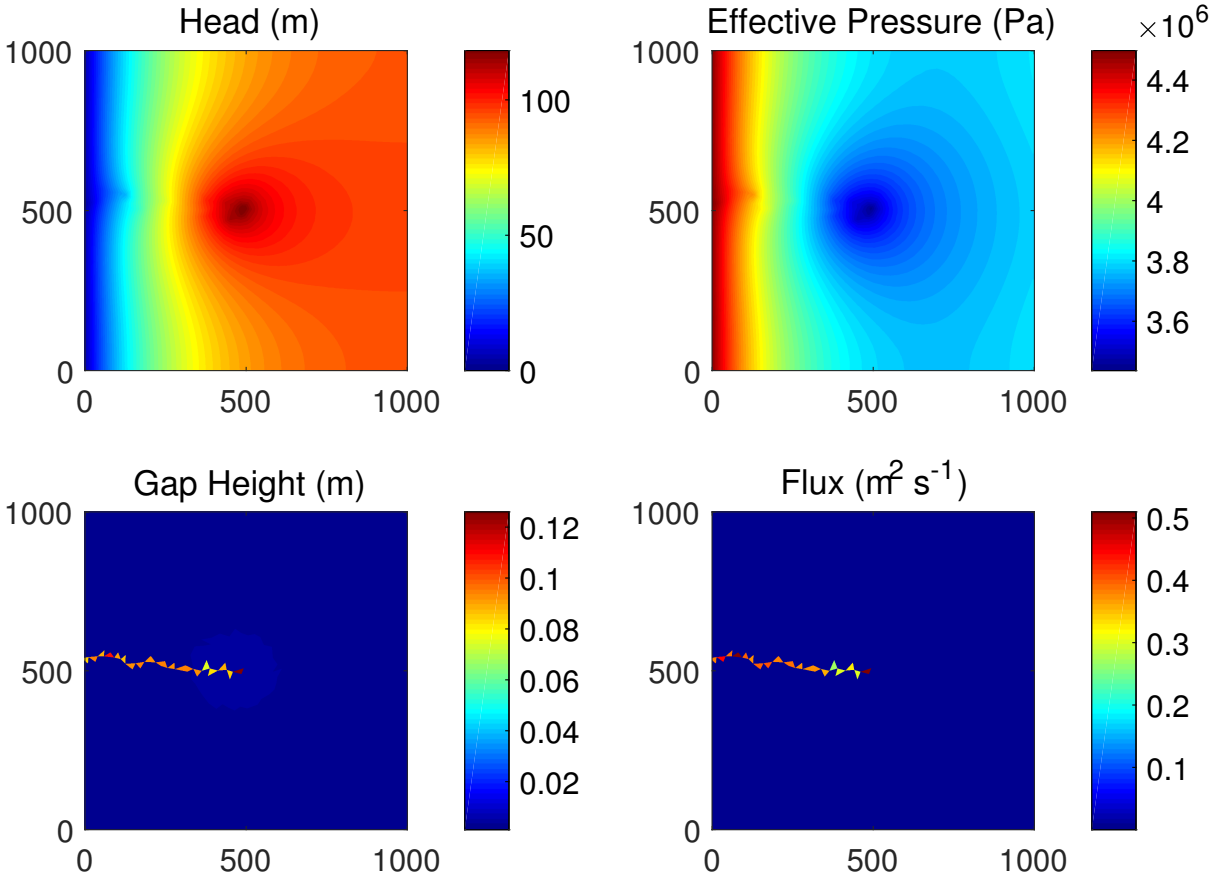

Figure 2. Steady configurations of hydraulic head, effective pressure, gap height, and depth-integrated basal water flux steady input of 4 m^3 s^{-1} into a moulin at the center of a 1 km square domain. Ice thickness is 500 m, with surface and bed slope of 0.02. The simulation was run to steady state with a time step of 900 s, and a clear efficient channel pathway forms from the moulin input to the outflow at the left edge of the domain, characterized by lower head, and higher effective pressure, gap height, and flux than its surroundings.

Geosci. Model Dev. Discuss., https://doi.org/10.5194/gmd-2018-58
Manuscript under review for journal Geosci. Model Dev.
Discussion started: 27 March 2018

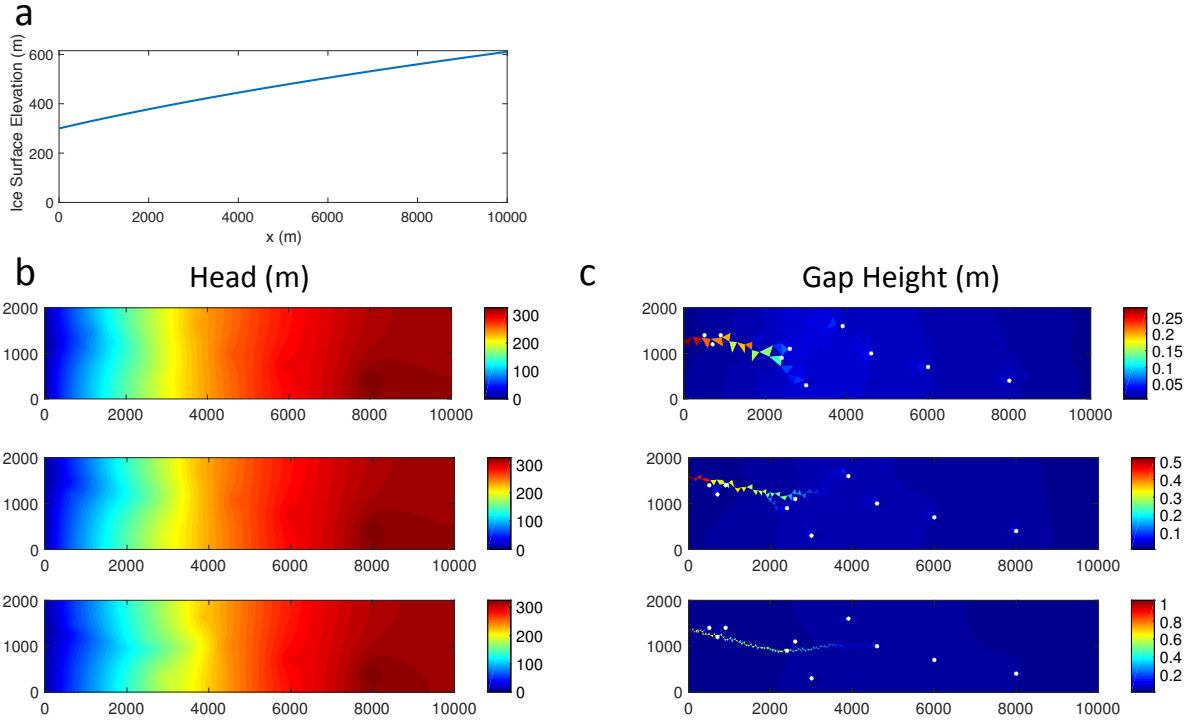

Figure 3. (a) Parabolic surface profile (uniform in the y direction) for a rectangular test domain with a flat bed. Ice thickness goes from 300 m at the outflow (x=0) to 610 m at x=1,000 m. (b) Steady-state head and (c) gap height distributions resulting from steady input of 10 $m^3\ s^{-1}$ into 10 moulins placed arbitrarily throughout the domain. Moulin locations are indicated on the gap height plots as white markers. Rather than each moulin forming an independent channel, the various inputs warp the pressure field and interact to produce a principal efficient drainage pathway. As a qualitative evaluation of mesh dependence, results are shown for typical element side lengths of 200 m, 100 m, and 50 m. While the gap height geometry across each element is dependent on mesh size, the head, water pressure, and effective pressure are similar for all cases.

Geosci. Model Dev. Discuss., https://doi.org/10.5194/gmd-2018-58
Manuscript under review for journal Geosci. Model Dev.
Discussion started: 27 March 2018

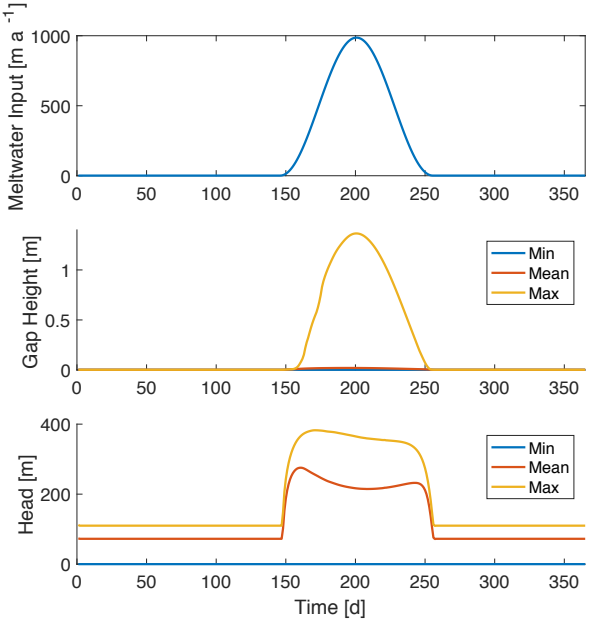

Figure 4. (a) Seasonal cycle of distributed meltwater input over one annual cycle. (b) Gap height evolution. As meltwater input increases, the maximum gap height increases, then decreases simultaneously with the decrease in input. (c) Head evolution. As meltwater input increases, the head increases, then decreases as channels are established (corresponding to lower water pressure in the efficient channel pathways, as well as lower head in the unchannelized upstream regions as shown in Fig. 5). As melt decreases, mean head increases again as the channels start to collapse, then decreases as melt returns to the winter minimum.

Geosci. Model Dev. Discuss., https://doi.org/10.5194/gmd-2018-58
Manuscript under review for journal Geosci. Model Dev.
Discussion started: 27 March 2018

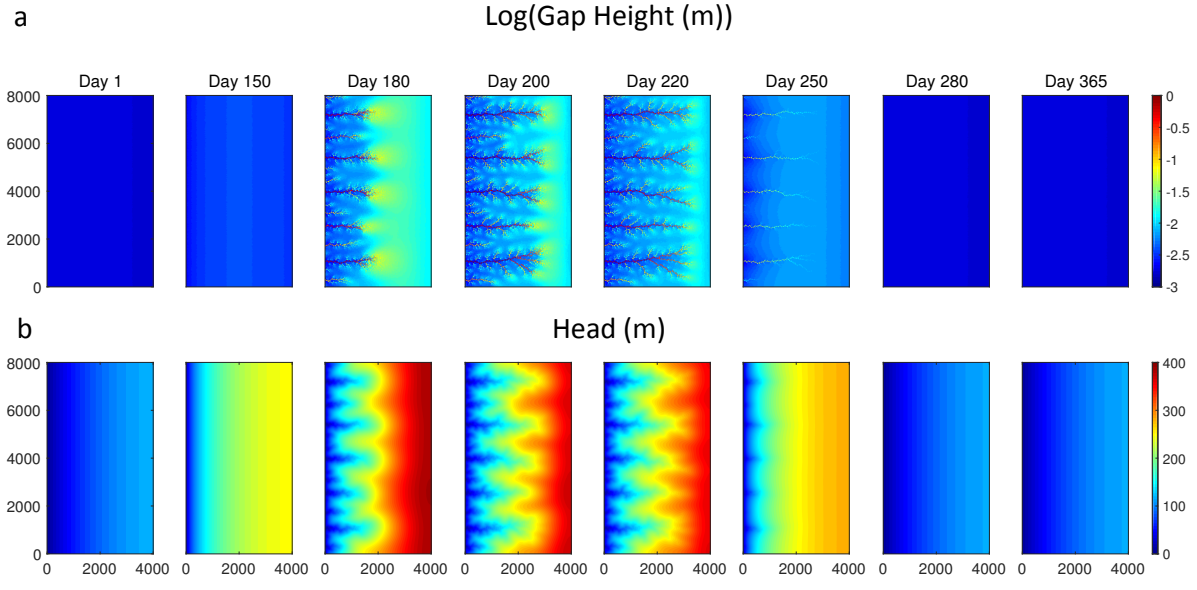

Figure 5. Seasonal evolution with distributed meltwater input as shown in Fig. 4 on a 4 km by 8 km domain. (a) Log (base 10) of gap height over one full annual cycle. Self-organized channels form from the outflow (left edge of the domain) as melt input increases, persist through the melt season, and collapse again as melt input decreases, returning to a steady sheet configuration. (b) Corresponding head distribution over one full annual cycle. The channels show lower head (i.e. higher effective pressure) than their surrounding areas in the y direction.

Geosci. Model Dev. Discuss., https://doi.org/10.5194/gmd-2018-58
Manuscript under review for journal Geosci. Model Dev.
Discussion started: 27 March 2018

Geoscientific Model Development Discussions
Open Access
EGU

Table 1. Variables used in model equations

Symbol	Units	Description
b	m	Subglacial gap height (average over element)
b_e	m	Englacial storage volume per unit area of bed, $b_e = e_v(h - z_b)$
t	s	Time
$\boldsymbol{q}$	$m^2\ s^{-1}$	Gap-integrated basal water flux
$\dot{m}$	$kg\ m^{-2}\ s^{-1}$	Internal melt rate
p_i	Pa	Ice overburden pressure, $p_i = \rho_i g H$
p_w	Pa	Subglacial water pressure, $p_w = \rho_w g(h - z_b)$
Re	Dimensionless	Reynolds number, $\mathrm{Re} = \lvert\boldsymbol{q}\rvert/\nu$
h	m	Hydraulic head
β	Dimensionless	Parameter to control opening due to sliding over bedrock bumps, $\beta = (b_r - b)/l_r$ for $b < b_r$, $\beta = 0$ for $b \geq b_r$
N	Pa	Effective pressure, $N = p_i - p_w$

Geosci. Model Dev. Discuss., https://doi.org/10.5194/gmd-2018-58
Manuscript under review for journal Geosci. Model Dev.
Discussion started: 27 March 2018

Geoscientific Model Development Discussions
Open Access
EGU

Table 2. Constants and parameters

Symbol	Value	Units	Description
ρ_w	1,000	kg m^{-3}	Bulk density of water
$i_{e \rightarrow b}$		m s^{-1}	Input rate of meltwater from englacial system to subglacial system
ρ_i	910	kg m^{-3}	Bulk density of ice
A		Pa^{-3} s^{-1}	Flow law parameter
n	3	Dimensionless	Flow law exponent
b_r	0.1	m	Typical height of bed bumps
l_r	2.0	m	Typical spacing between bed bumps
u_b	10^{-6}	m s^{-1}	Sliding velocity
g	9.8	m s^{-2}	Gravitational acceleration
ω	0.001	Dimensionless	Parameter controlling nonlinear transition between laminar and turbulent flow
L	3.34×10^5	J kg^{-1}	Latent heat of fusion of water
G	0.05	W m-2	Geothermal flux
c_t	7.5×10^{-8}	K Pa^{-1}	Change of pressure melting point with temperature
c_w	4.22×10^3	J kg^{-1} K^{-1}	Heat capacity of water
ν	1.787×10^-6	m^2 s^{-1}	Kinematic viscosity of water
e_v		Dimensionless	Englacial void ratio